



**Get Clarity On Generics**

Cost-Effective CT & MRI Contrast Agents

**FRESENIUS  
KABI**

[WATCH VIDEO](#)

**AJNR**

## **Hypothalamic Pilomyxoid Astrocytoma in a Child with Lipodystrophy**

J.C. Benson, J. Trejo-Lopez, S.E. Bach, J. Schwartz, T.J. Kaufmann, L. Eckel and J. Guerin

*AJNR Am J Neuroradiol* 2021, 42 (8) 1370-1374

doi: <https://doi.org/10.3174/ajnr.A7136>

<http://www.ajnr.org/content/42/8/1370>

This information is current as  
of August 21, 2025.

# Hypothalamic Pilomyxoid Astrocytoma in a Child with Lipodystrophy

 J.C. Benson,  J. Trejo-Lopez,  S.E. Bach,  J. Schwartz,  T.J. Kaufmann,  L. Eckel, and  J. Guerin

## ABSTRACT

**SUMMARY:** Pilomyxoid astrocytoma is a rare form of pediatric CNS malignancy first classified in 2007 by the World Health Organization. The tumors are similar to pilocytic astrocytomas, sharing both some imaging and histologic traits. However, pilomyxoid astrocytomas portend a more ominous prognosis, with more aggressive local tendencies and a greater proclivity for leptomeningeal spread. Although tissue sampling is ultimately required to differentiate pilocytic astrocytomas and pilomyxoid astrocytomas, some imaging features can be used to suggest a pilomyxoid astrocytoma, including homogeneous enhancement, leptomeningeal seeding, and lack of intratumoral cysts. In this article, a case of a hypothalamic pilomyxoid astrocytoma is described, in which the presenting disorder was profound generalized lipodystrophy. The aforementioned imaging characteristics of pilomyxoid astrocytomas are reviewed, as are the pathologic features of such tumors, including their angiocentric cellular arrangement and myxoid background.

**ABBREVIATION:** PMA = pilomyxoid astrocytoma

The patient was a 2-year-old boy who presented with a history of poor weight gain with loss of adipose tissue despite normal growth in height during the previous 12 months. His symptoms ultimately culminated in hospitalization for failure to thrive. Physical examination revealed a scarcity of subcutaneous fat with relative prominence of his musculature and vasculature (Fig 1). A comprehensive genetic screen for congenital lipodystrophy performed at an outside institution had negative findings. Given the association between CNS tumors and generalized lipodystrophy, the patient's endocrinologist requested a brain MR imaging to assess an intracranial mass.

## Imaging

MR imaging demonstrated a well-circumscribed lobulated mass arising from the hypothalamic/optic chiasmatic region, measuring up to 3.0 cm in maximum diameter. Intralesional signal was uniformly hyperintense on T2-weighted and FLAIR images and was prominently hypointense on T1-weighted images. The mass avidly and uniformly enhanced following contrast administration.

Displacement occurred in adjacent structures: The optic chiasm and pituitary infundibulum were pushed anteriorly, the midbrain was deviated dorsally, and the optic tracts draped around the lateral aspects of the mass. Inferiorly, the mass extended into both the suprasellar and prepontine cisterns (Fig 2), and the lesion extended superiorly into the third ventricle. Remote from the mass were a few smaller enhancing lesions along the surface of the right temporal lobe, medulla, and cerebellum, consistent with leptomeningeal spread. Imaging of the remainder of the neuraxis revealed several additional enhancing foci along the thoracic spinal cord and cauda equina, concerning for additional leptomeningeal tumor dissemination (Fig 3).

The imaging characteristics were thought to be consistent with a hypothalamic glioma, either a pilocytic astrocytoma or a pilomyxoid astrocytoma (PMA). The diffuse leptomeningeal seeding seen along the neuraxis is more common in PMA. Other tumors typically found in this region were less likely. For example, germinomas more frequently demonstrate intratumoral cysts and restricted diffusivity, hypothalamic hamartomas lack enhancement, and neither craniopharyngiomas nor gangliogliomas are expected to have diffuse subarachnoid seeding.

## Subsequent Clinical Course

On the basis of imaging characteristics of a probable low-grade glioma and the expected risk of morbidity associated with surgical biopsy, the decision was made to forgo pathologic sampling in favor of a chemotherapy regimen. The patient was treated with

Received December 30, 2020; accepted after revision February 16, 2021.

From the Departments of Radiology (J.C.B., T.J.K., L.E., J.G.), Laboratory Medicine and Pathology (J.T.-L.), and Pediatric and Adolescent Medicine (J.S.), Mayo Clinic, Rochester, Minnesota; and Department of Laboratory Medicine and Pathology (S.E.B.), OSF Saint Francis Medical Center, Peoria, Illinois.

Please address correspondence to John C. Benson, MD, 723 6th St. SW, Department of Radiology, Mayo Clinic, Rochester, MN 55902; e-mail: benson.john3@mayo.edu  
<http://dx.doi.org/10.3174/ajnr.A7136>



**FIG 1.** Photographs of the patient demonstrate clinical sequelae of lipodystrophy, with profound loss of subcutaneous fat. Printed with authorization from the patient's parents.

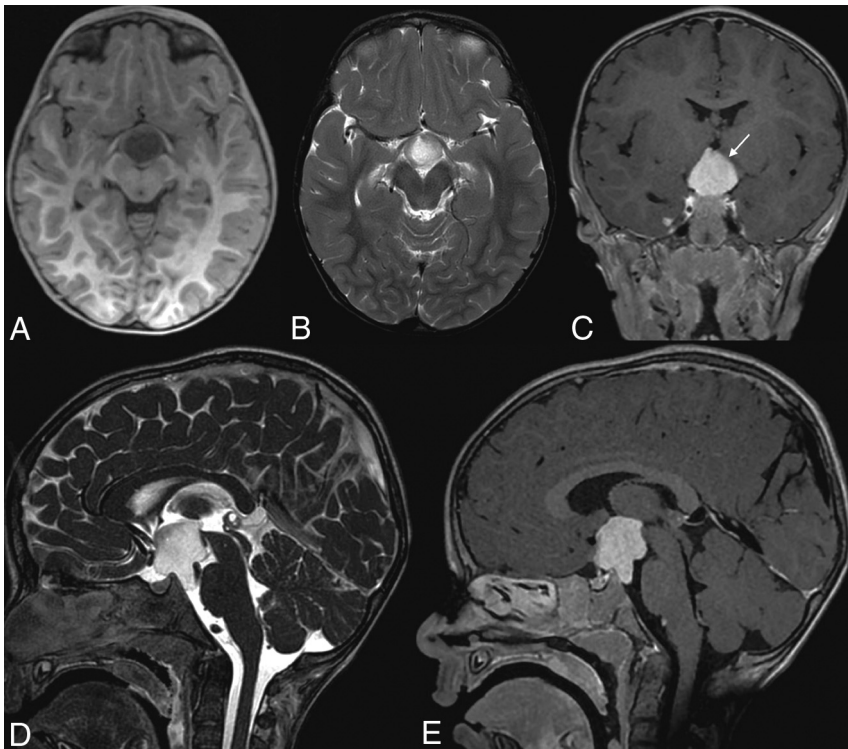


**FIG 2.** Tumor appearance on axial MPRAGE (A) and T2WI (B), coronal postgadolinium T1-weighted Cube (GE Healthcare) (C), and sagittal FIESTA (D) and postgadolinium T1-weighted Cube (E). Images demonstrate an enhancing lobulated mass arising from the hypothalamic/chiasmatic region, with indistinct borders between the tumor and adjacent left hypothalamic parenchyma (arrow).

vincristine and carboplatin, the current standard of care for patients with low-grade gliomas (single lesion or multifocal) that are not amenable to surgical resection.

MR imaging performed approximately 3 months after chemotherapy initiation demonstrated a slight increase in size of the primary hypothalamic tumor, measuring 1.9 cm in the

maximum axial diameter along its superior margin compared with 1.5 cm on the initial examination. Partially related to travel restrictions at the time of the coronavirus disease 2019 pandemic, the patient continued his care at an outside facility with continued consultation from our institution. A radiologist's interpretation of a follow-up MR imaging, performed at the outside hospital, expanded the differential to include craniopharyngioma and metastasis. Because of concerns related to diagnostic uncertainty and apparent lack of response to treatment, a biopsy was performed.

### Pathology

Histologic examination of the tumor revealed a population of overall monomorphous neoplastic cells embedded in a myxoid background and demonstrating prominent angiocentric arrangements (Fig 4). No substantial mitotic activity, necrosis, or microvascular proliferation was identified in the material, histologically supporting a low-grade neoplasm.

Immunohistochemical studies revealed tumor cells diffusely and strongly reactive for glial fibrillary acidic protein, consistent with glioma, as opposed to nonglial processes such as germ cell tumor, lymphoma, and metastatic disease. A neurofilament study revealed, overall, few axons in the tumor background; this finding was compatible with an expansile rather than infiltrative growth pattern, a feature seen in noninfiltrative tumors such as pilocytic astrocytoma, and less consistent with tumors characterized by extensive infiltrative growth such as diffuse astrocytoma and oligodendroglioma. Also inconsistent with these latter entities, neoplastic cells were negative for the *IDH1 R132H* mutation on surrogate immunohistochemistry. By current 2016 World Health Organization criteria, the definitive diagnosis of oligodendroglioma requires the identification of

both an isocitrate dehydrogenase (*IDH*) mutation as well as whole-arm chromosomal codeletion of 1p and 19q.<sup>1</sup> *IDH* mutations also define a category of infiltrating astrocytoma commonly arising in younger adults; such *IDH*-mutant astrocytomas commonly also have mutations of *ATRX* and *p53*, though these mutations are not required for the diagnosis.<sup>2</sup>

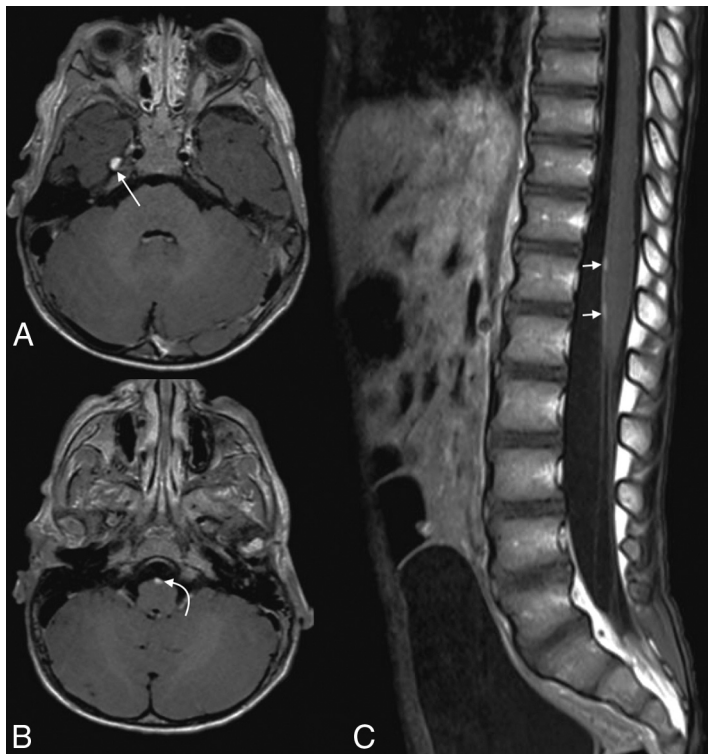


**FIG 3.** Leptomeningeal seeding seen on axial postgadolinium T1 Cube (A and B) and sagittal postgadolinium T1 images of the lower spine (C). Multiple enhancing foci are noted, including along the right temporal lobe (long straight arrow in A), ventral medulla (curved arrow in B), and ventral conus medullaris (short straight arrows in C). There is near-complete absence of subcutaneous fat, compatible with the patient's known lipodystrophy.

While the tumor was negative for the *BRAF* V600E mutation by immunohistochemistry, fluorescence in situ hybridization studies revealed that the tumor had a duplication of *BRAF* (at the 7q34 chromosome locus), an alteration that serves as a surrogate for the detection of *KIAA1549-BRAF* fusion. This latter fusion alteration is a well-described molecular event in pilocytic astrocytoma and its histologic variant, PMA. Pilocytic astrocytoma is classically described as a glioma exhibiting a biphasic histologic pattern, with compact areas of bipolar cells containing Rosenthal fibers and eosinophilic granular bodies alternating with areas of loose-textured background containing multipolar cells and microcysts. PMA is histologically differentiated from classic pilocytic astrocytoma by angiocentric arrangements of bipolar tumor cells, as well as the presence of a markedly myxoid background, a morphologic appearance well-represented by this neoplasm and thus favoring this diagnosis.

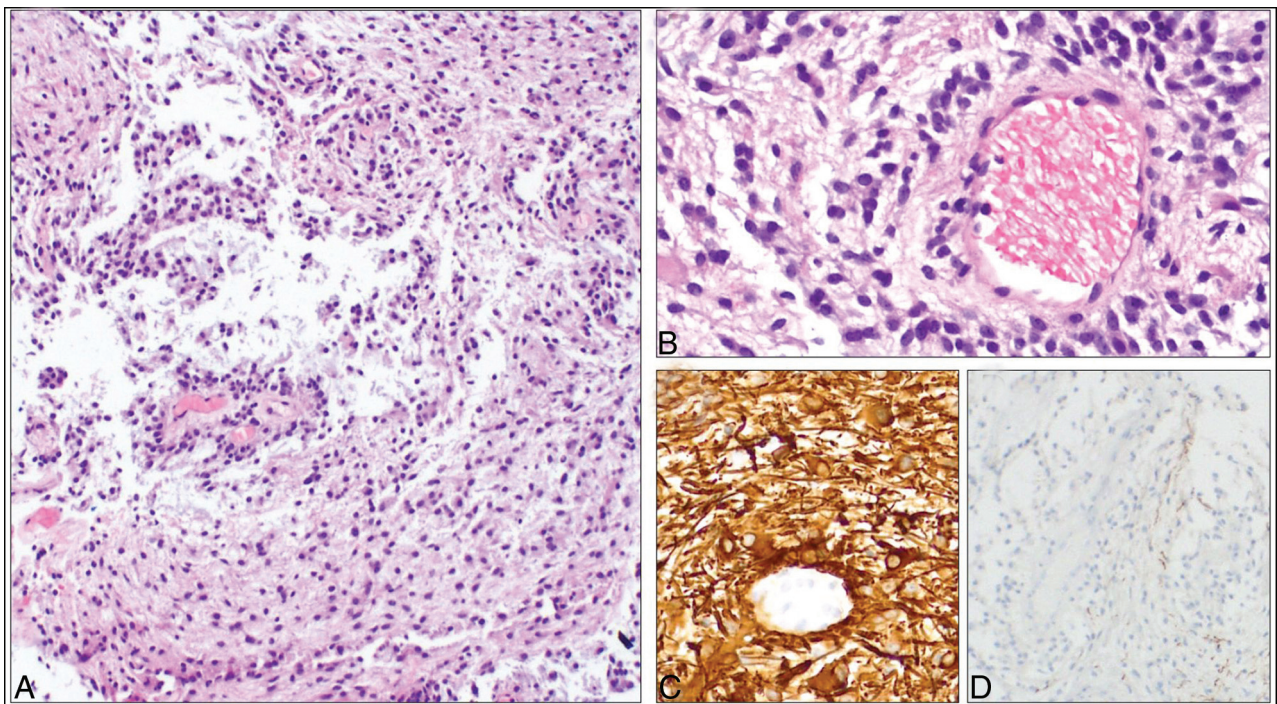


**FIG 4.** Photomicrographs of the tumor reveal a glioma composed of overall monotonous neoplastic cells embedded in a myxoid background (A, H&E,  $\times 100$  magnification) and exhibiting prominent angiocentric arrangements (B, H&E,  $\times 200$  magnification). Neoplastic cells demonstrate immunoreactivity for glial fibrillary acidic protein. C, Glial fibrillary acidic protein immunohistochemistry,  $\times 200$  magnification. Neurofilament reveals, overall, few background axons, compatible with a predominantly expansile growth pattern (D, neurofilament immunohistochemistry,  $\times 100$  magnification).

## DISCUSSION

Pilomyxoid astrocytomas are rare pediatric CNS tumors, accounting for approximately 2% of childhood astrocytomas.<sup>3</sup> First introduced in 1999 and classified by the World Health Organization in 2007, PMAs were originally identified as a variant of pilocytic astrocytomas.<sup>4</sup> The discovery of PMAs partially helped explain what had been a baffling attribute of pilocytic astrocytomas: Though most exhibited indolent growth and favorable prognoses, a subset of pilocytic astrocytomas demonstrated unexpected aggressiveness. PMAs fit nicely into this diagnostic puzzle, offering an explanation for the observed clinical variability.<sup>5</sup> Patients with PMAs have higher rates of local recurrence and CSF dissemination and shorter progression-free and overall survival than those with pilocytic astrocytomas.<sup>6,7</sup>

Given the variability of its clinical behavior and prognosis, in 2007, the World Health Organization had classified this tumor as a grade II disease. However, in its 2016 classification, they removed the grade assignments to PMAs.<sup>5</sup> PMAs typically occur in younger patients; an average age of onset for PMAs is 18 months, compared with 58 months for pilocytic astrocytomas, leading to early labels of an “infantile” subtype.<sup>4,6</sup> However, cases have been identified across a broad age range, even among adults.<sup>8</sup> Clinical presentations vary and include developmental delay, failure to thrive, vomiting, feeding difficulties, and generalized weakness.<sup>6</sup> In infants, the initial clinical manifestations can be more subtle, such as increased head size or bulging fontanelle from increased intracranial pressure.<sup>5</sup>

On imaging, PMAs have an idiosyncratic proclivity for the hypothalamic/chiasmatic region (60%–75% of cases), though they may occur anywhere along the neuraxis, particularly the cerebral hemispheres.<sup>9,10</sup> The tumors are typically well-circumscribed, predominantly solid tumors, with high homogeneous

intralesional signal on T2-weighted and T2-weighted FLAIR images and iso- to hypointense signal on T1-weighted imaging, reflecting their myxoid matrix (Fig 5).<sup>9</sup> The reported frequency of central necrosis varies; some authors believe it to be rare, while a large review of cases noted necrosis in nearly one-third of tumors.<sup>8,11</sup> Peritumoral edema is infrequently seen.<sup>12</sup> PMAs tend to be devoid of calcifications and do not demonstrate reduced diffusivity, helping distinguish them from craniopharyngiomas and germinomas, respectively.<sup>12</sup> Obstructive hydrocephalus may be present, though usually in a minority of patients.<sup>5</sup>

Prior studies have sought to distinguish between PMAs and pilocytic astrocytomas on the basis of imaging features. In general, PMAs demonstrate more homogeneous enhancement, are more susceptible to intratumoral hemorrhage, and are less prone to intralesional cystic changes (Table).<sup>12,13</sup> PMAs are also more prone to leptomeningeal spreading, occurring in approximately 20% of tumors in 1 study; none of the pilocytic astrocytomas in the same study demonstrated such spread.<sup>6</sup> However, considerable overlap exists between the entities. Even in the hypothalamic/chiasmatic region, most pediatric low-grade tumors are pilocytic astrocytomas.<sup>6</sup> In this area, about 20%–50% of pilocytic astrocytomas are associated with neurofibromatosis type 1.<sup>14,15</sup> Fernandez et al<sup>11</sup> found a higher rate of intratumoral necrosis in PMAs—not surprising, given their relative aggressiveness—though this has not been reported elsewhere. Alkonyi et al<sup>12</sup> found no difference in the size, margins, or intralesional T1 and T2 signal characteristics between PMAs and pilocytic astrocytomas. Ultimately, in its most classic form, a solid hypothalamic mass with leptomeningeal spread in a young pediatric patient, imaging alone might help favor a PMA over a pilocytic astrocytoma. Nevertheless, pathologic analysis is still required to confidently make such a distinction.<sup>16</sup>

The tumor in this case was discovered because of the astute diagnostic capabilities of the patient’s endocrinologist. Although rare, the connection between hypothalamic astrocytomas and lipodystrophy has been long known.<sup>17</sup> In its original description, “diencephalic syndrome” is characterized by emaciation, normal linear growth, locomotor overactivity, and somewhat incongruous pleasantness and euphoria.<sup>18,19</sup> However, many afflicted patients present with isolated lipodystrophy.<sup>20</sup> The mechanism by which hypothalamic astrocytoma results in such a profound loss of subcutaneous fat remains uncertain. Some authors have opined that the pathophysiology may be paraneoplastic, in which either antiadipocyte autoantibodies induce cytotoxicity or hormones/cytokines induce lipolysis. Others have suggested that growth hormone dysregulation and resistance may play a role. Regardless, the symptoms have been described in the setting of both pilocytic (and anaplastic) astrocytomas and PMAs.<sup>21,22</sup> It

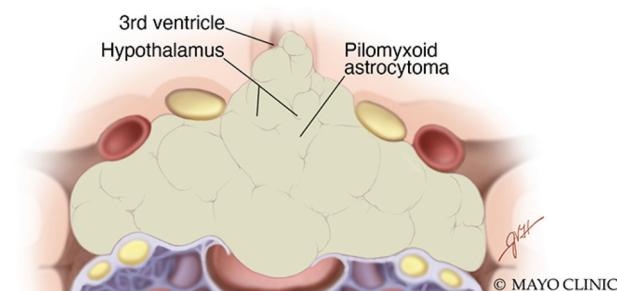


**FIG 5.** Artistic illustration of a PMA extending from the hypothalamus, with involvement of the suprasellar region and adjacent structures. PMAs tend to be solid and are typically devoid of both calcifications and intratumoral cysts. Used with permission of Mayo Foundation for Medical Education and Research. All rights reserved.

### Comparison of typical PMA and pilocytic astrocytoma clinical and imaging features

	PMA	Pilocytic Astrocytoma
Age	Younger (mean age, 1.5 yr)	Older (mean age, 4.8 yr)
Location	Hypothalamic/chiasmatic region	Cerebellum > hypothalamic/chiasmatic region
Enhancement	Homogeneous	Heterogeneous
Intratumoral contents	Most solid, with minimal tumoral cysts	Most have cystic content
Intratumoral hemorrhage	12%–25%	1%–8%
Evidence of leptomeningeal seeding	More frequent (up to 20%)	Exceedingly rare

remains unknown whether certain types of hypothalamic tumor, eg, PMA or pilocytic astrocytoma, are particularly prone to causing sequelae of the diencephalic syndrome.

The patient presented here recently completed his chemotherapy regimen of vincristine and carboplatin and had decreased tumor size on his most recent examination, measuring 1.9 cm in maximum axial diameter compared with 2.2 cm when at its largest size. Serial MRIs will be used to continue to observe the tumor. Currently, his prognosis is considered guarded-but-favorable, particularly given the recent decrease in tumor size. Nevertheless, the patient's body weight continues to be suboptimal. Although his family has reported that he is able to gain some weight during intermittent breaks in chemotherapy, it tends to fall off following re-initiation of treatment, and he continues to exhibit considerable symptoms of lipodystrophy.

### Case Summary

- Generalized lipodystrophy may be caused by a hypothalamic glioma. In its classic form, the clinical presentation includes additional elements of diencephalic syndrome: emaciation, euphoria, and locomotor hyperactivity.
- PMAs typically arise from the hypothalamic/chiasmatic region but may appear anywhere along the neuraxis.
- Pathologic confirmation is required for diagnosis, though radiographically, a PMA may be suggested over pilocytic astrocytoma when a solid composition, homogeneous enhancement, and leptomeningeal seeding are present.
- Histologically, PMA is currently defined by the 2016 World Health Organization as a variant of pilocytic astrocytoma, exhibiting a prominent myxoid background and perivascular arrangement of tumor cells, and demonstrates molecular alterations similar to those of classic pilocytic astrocytoma (including *KIAA1549-BRAF* fusion).

### REFERENCES

1. Louis DN, Perry A, Reifenberger G, et al. **The 2016 World Health Organization Classification of Tumors of the Central Nervous System: a summary.** *Acta Neuropathol* 2016;131:803–20 [CrossRef Medline](#)
2. Kannan K, Inagaki A, Silber J, et al. **Whole-exome sequencing identifies ATRX mutation as a key molecular determinant in lower-grade glioma.** *Oncotarget* 2012;3:1194–1203 [CrossRef Medline](#)
3. Stiller CA, Bayne AM, Chakrabarty A, et al. **Incidence of childhood CNS tumours in Britain and variation in rates by definition of malignant behaviour: population-based study.** *BMC Cancer* 2019;19:139 [CrossRef Medline](#)
4. Tihan T, Fisher PG, Kepner JL, et al. **Pediatric astrocytomas with monomorphous pilomyxoid features and a less favorable outcome.** *J Neuropathol Exp Neurol* 1999;58:1061–68 [CrossRef Medline](#)
5. Burger PC, Khandji AG, Tihan T, et al. **Pilomyxoid astrocytoma: a review.** *Medscape Gen Med* 2004;6:42. <https://www.ncbi.nlm.nih.gov/pmc/articles/PMC1480592/>. Accessed October 9, 2020
6. Komotar RJ, Burger PC, Carson BS, et al. **Pilocytic and pilomyxoid hypothalamic/chiasmatic astrocytomas.** *Neurosurgery* 2004;54:72–80; discussion 79–80 [CrossRef Medline](#)
7. Lee IH, Kim JH, Suh YL, et al. **Imaging characteristics of pilomyxoid astrocytomas in comparison with pilocytic astrocytomas.** *Eur J Radiol* 2011;79:311–16 [CrossRef Medline](#)
8. Pruthi SK, Chakraborti S, Naik R, et al. **Pilomyxoid astrocytoma with high proliferation index.** *J Pediatr Neurosci* 2013;8:243–46 [CrossRef Medline](#)
9. Arslanoglu A, Cirak B, Horska A, et al. **MR imaging characteristics of pilomyxoid astrocytomas.** *AJNR Am J Neuroradiol* 2003;24:1906–08 [Medline](#)
10. Ho CY, Supakul N, Patel PU, et al. **Differentiation of pilocytic and pilomyxoid astrocytomas using dynamic susceptibility contrast perfusion and diffusion weighted imaging.** *Neuroradiology* 2020;62:81–88 [CrossRef Medline](#)
11. Fernandez C, Figarella-Branger D, Girard N, et al. **Pilocytic astrocytomas in children: prognostic factors—a retrospective study of 80 cases.** *Neurosurgery* 2003;53:544–553; discussion 554–55 [CrossRef Medline](#)
12. Alkonyi B, Nowak J, Gnekow AK, et al. **Differential imaging characteristics and dissemination potential of pilomyxoid astrocytomas versus pilocytic astrocytomas.** *Neuroradiology* 2015;57:625–38 [CrossRef Medline](#)
13. White JB, Piepgras DG, Scheithauer BW, et al. **Rate of spontaneous hemorrhage in histologically proven cases of pilocytic astrocytoma.** *J Neurosurg* 2008;108:223–26 [CrossRef Medline](#)
14. Poussaint TY. **Magnetic resonance imaging of pediatric brain tumors: state of the art.** *Top Magn Reson Imaging* 2001;12:411–33 [CrossRef Medline](#)
15. Plaza MJ, Borja MJ, Altman N, et al. **Conventional and advanced MRI features of pediatric intracranial tumors: posterior fossa and suprasellar tumors.** *AJR Am J Roentgenol* 2013;200:1115–24 [CrossRef Medline](#)
16. Karthigeyan M, Singhal P, Salunke P, et al. **Adult pilomyxoid astrocytoma with hemorrhage in an atypical location.** *Asian J Neurosurg* 2019;14:300–03 [CrossRef Medline](#)
17. Fleischman A, Brue C, Poussaint TY, et al. **Diencephalic syndrome: a cause of failure to thrive and a model of partial growth hormone resistance.** *Pediatrics* 2005;115:e742–48 [CrossRef Medline](#)
18. British Paediatric Association. **Proceedings of the twenty-second general meeting of the British Pediatric Association.** *Arch Dis Child* 1951;26:270–25 [CrossRef](#)
19. Addy DP, Hudson FP. **Diencephalic syndrome of infantile emaciation.** *Arch Dis Child* 1972;47:338–43 [CrossRef Medline](#)
20. Patni N, Alves C, von Schnurbein J, et al. **A novel syndrome of generalized lipodystrophy associated with pilocytic astrocytoma.** *J Clin Endocrinol Metab* 2015;100:3603–06 [CrossRef Medline](#)
21. Singh G, Wei XC, Hader W, et al. **Sustained response to weekly vinblastine in 2 children with pilomyxoid astrocytoma associated with diencephalic syndrome.** *J Pediatr Hematol Oncol* 2013;35:e53–56 [CrossRef Medline](#)
22. Stival A, Lucchesi M, Farina S, et al. **An infant with hyperalertness, hyperkinesia, and failure to thrive: a rare diencephalic syndrome due to hypothalamic anaplastic astrocytoma.** *BMC Cancer* 2015;15:616 [CrossRef Medline](#)